Quaternary Science Reviews 57 (2012) 46–57

Contents lists available at SciVerse ScienceDirect

Quaternary Science Reviews

journal homepage: www.elsevier.com/locate/quascirev

The influence of sub-glacial bed evolution on ice extent: a model-based evaluation of the Last Glacial Maximum Pukaki glacier, New Zealand

Karen A. McKinnon [a,b,*], Andrew N. Mackintosh [b], Brian M. Anderson [b], David J.A. Barrell [c]

[a] Harvard University, Earth and Planetary Sciences, 20 Oxford St., Cambridge, MA 02138, USA
[b] Victoria University of Wellington, Antarctic Research Centre, PO Box 600, Wellington 6140, New Zealand
[c] GNS Science, 764 Cumberland Street, Dunedin 9054, New Zealand

ARTICLE INFO

Article history:
Received 2 April 2012
Received in revised form
27 September 2012
Accepted 1 October 2012
Available online 30 October 2012

Keywords:
Glacier bed profiles
Glacier modeling
Paleoclimate
New Zealand
Last Glacial Maximum

ABSTRACT

A potential complication in using glacier extent to estimate paleoclimatic conditions is the influence of glacier bed evolution on changes in ice extent over time. Here, we examine this issue through model-based reconstructions of the Last Glacial Maximum (LGM) Pukaki glacier, Southern Alps, New Zealand, whose LGM extents are exceptionally well defined by lateral and terminal moraines. Using the well-dated moraine limits as an empirical constraint on maximum ice extents, we employ a one-dimensional glacier flowline model driven by a mass balance model in order to evaluate the influence of climate and glacier bed profile on the extent of the LGM Pukaki glacier. The LGM glacier bed is buried by Lateglacial and post-glacial sediment, so we calculate bed profiles using a modified version of the one-dimensional model and available geologic constraints. A best fit to the moraine record occurs with a LGM temperature of 7–8 °C cooler than present, with precipitation ranging from 80% to 100% of present levels. Modeling of the bed profile evolution indicates that bed changes alone could account for kilometer-scale changes in glacier width and length.

1. Introduction

New Zealand occupies a climatically sensitive geographical position, at the interfaces between the southwest Pacific Ocean and the Southern Ocean, and between the subtropical high-pressure belt and the mid-latitude westerlies. This makes records of past climatic variability from the New Zealand region particularly valuable for offering insights into past climate dynamics on large spatial scales, which in turn informs understanding of global climatic sensitivity and helps to constrain scenarios of future climate (e.g. Solomon et al., 2007).

There is a growing understanding of Last Glacial Maximum (LGM) climate patterns in and around New Zealand derived from a variety of proxies, as summarized in Alloway et al. (2007). In the marine realm, knowledge of oceanic conditions comes from foraminiferal (Weaver et al., 1998; Sikes et al., 2002; Barrows and Juggins, 2005; Samson et al., 2005), alkenone (Sikes et al., 2002), and Mg/Ca ratio (Pahnke et al., 2003) studies. Terrestrial climate history has to a large extent been based on paleoecological proxies including beetle fauna (Marra et al., 2006) and pollen flora (Shulmeister et al., 2001; Sandiford et al., 2003; Wilmshurst et al., 2007), but recent progress in the high-precision dating of glacier landforms has greatly increased the value of glaciological proxies for paleoclimatic reconstructions in New Zealand (Kaplan et al., 2010; Barrell, 2011). Recent regional-scale modeling of the LGM ice field of the Southern Alps (Golledge et al., 2012) found that a LGM cooling of 6–6.5 °C with a precipitation reduction of up to 25% from present was consistent with the mapped South Island LGM moraine record. Similar results, of a cooling of 6.25–7.0 °C with a precipitation reduction of up to 10%, were found through modeling a smaller region of three basins in the Southern Alps (Rowan et al., in press).

The Lake Pukaki catchment in the central Southern Alps, South Island, New Zealand (Fig. 1), contains an exceptionally well preserved geomorphological record of moraines (Porter, 1975) with progressively improving knowledge of the ages of these moraines (Schaefer et al., 2006, 2009; Putnam et al., 2010a,b). In this study, we use this well-resolved landform record as an empirical foundation for a simple coupled climate-glacier model of the LGM Pukaki glacier, which we employ to inquire into the relative influences of climate, as measured by temperature and precipitation, and glacier bed profile on the behavior of the LGM Pukaki glacier.

* Corresponding author. Harvard University, Earth and Planetary Sciences, 20 Oxford St., Cambridge, MA 02138, USA.
E-mail address: mckinnon@fas.harvard.edu (K.A. McKinnon).

0277-3791/$ – see front matter © 2012 Elsevier Ltd. All rights reserved.
http://dx.doi.org/10.1016/j.quascirev.2012.10.002

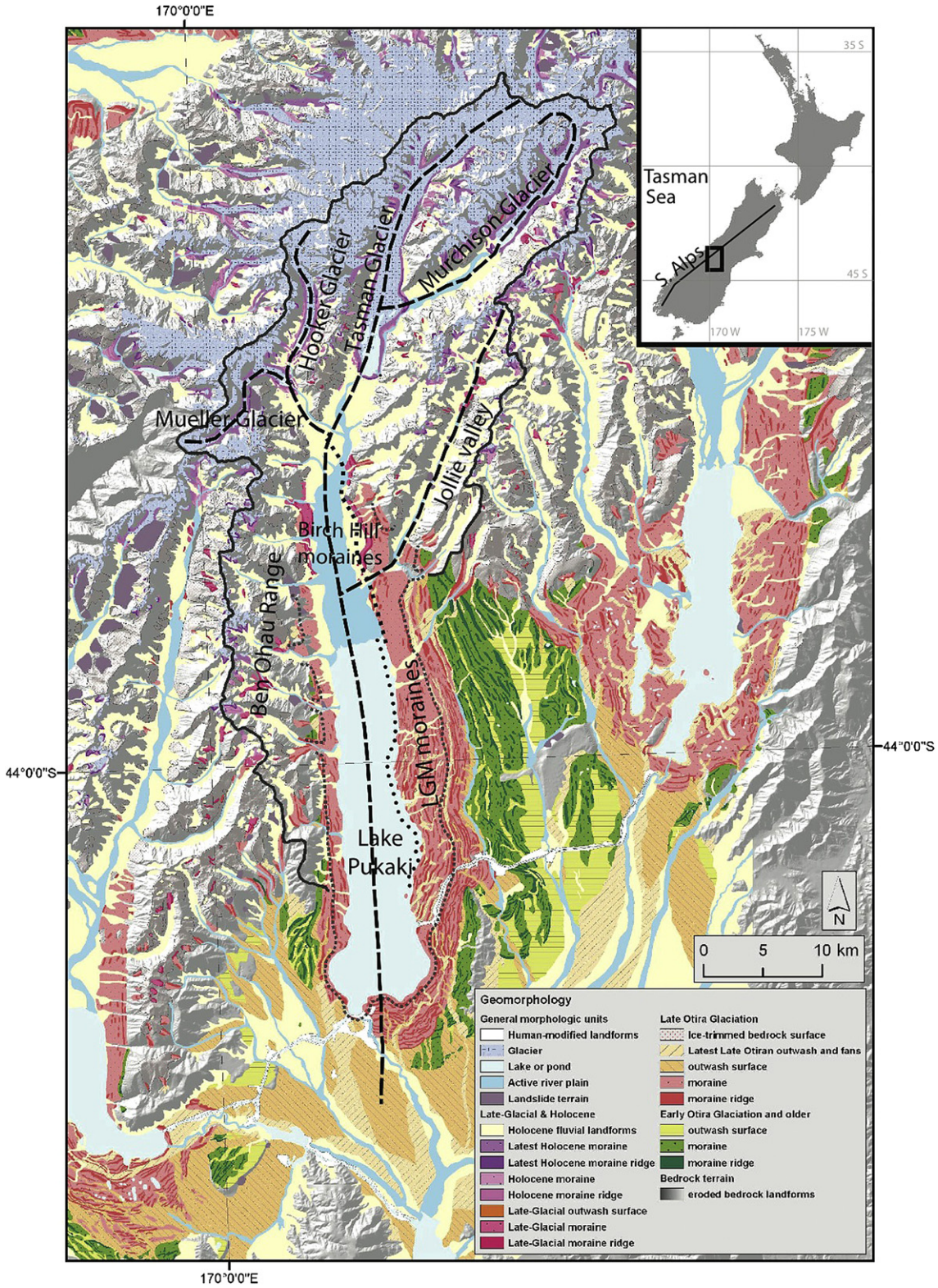

Fig. 1. The region of study, and the mapped moraines, adapted from Barrell et al. (2011). The black dashed lines are the flowlines used in modeling. Individual moraine ridges are marked in bold color. The thin solid line indicates the catchment boundary. The Late Otira Glaciation corresponds to the LGM; the outer limit of red moraines marks the early LGM glacier limit modeled here, while the thin dotted line denotes the late LGM glacier extent. The location of the seismic lines used to estimate bedrock location from Kleffmann et al. (1998) and Long et al. (2003) are shown via the circle and square markers, respectively. (For interpretation of the references to color in this figure legend, the reader is referred to the web version of this article.)

We consider two major glacier extents during the LGM. The outer, early LGM limit of Pukaki glacier is based on the maximum extent of LGM moraines from Barrell et al. (2011), which was modeled by Golledge et al. (2012). The inner, late LGM limit is closely aligned with the deglacial moraine line shown by Schaefer et al. (2006). It represents a refinement of the boundary between the locally-named 'Tekapo' and older 'Mt. John' moraine belts shown by Cox and Barrell (2007). The culmination of the Tekapo advance, followed by major glacier recession, was approximately 18 thousand years ago (ka), based on cosmogenic isotope dating near Boundary Stream on the western side of Lake Pukaki (Putnam et al., 2010b). Although further cosmogenic dating of the LGM moraine belts is in progress, results are not yet available, and in the interim we assume that the oldest LGM moraines correspond with the beginning of the LGM at approximately 28 ka, as indicated by other paleo-proxy data (Alloway et al., 2007).

One component of this study is to evaluate the early and late LGM climate state(s) consistent with the moraine record, but we differ from the regional-scale modeling of Golledge et al. (2012) in two ways.

First, we deliberately use a simple glacier model, based on the shallow ice approximation (SIA), and choose the domain of a single glacier in order to explore model sensitivity and prevent model over-fitting, given the small number of data constraints on our model. While there exists some concern that the SIA is not appropriate for modeling alpine glaciers due to their short horizontal length scales (Kamb and Echelmeyer, 1986; Le Meur et al., 2004; Hindmarsh, 2006) and relatively steep profiles (Baral et al., 2001), the SIA produces glacier responses to climatic changes that are very similar to those calculated from a more complete model for an idealized alpine glacier (Leysinger Vieli and Gudmundsson, 2004). It has also been used with success in modeling contemporary glacier advance and retreat in response to mass balance changes (e.g. Oerlemans et al., 1998).

Second, we specifically focus on the role of the bed profile in reconstructing glacier extent and change. Bed topography and composition are major controls on glacier behavior because (1) the sensitivity of glacier length to climate changes depends on bed slope (Oerlemans, 1989), (2) the surface elevation of the bed partly determines the temperature at the glacier terminus due to the negative atmospheric lapse rate, and (3) the properties of the substrate affect the dynamics of glacier flow (Truffer et al., 2001) and the resulting glacier surface longitudinal profile (Boulton and Jones, 1979). The relationship between glacier motion and erosion has primarily been studied with respect to a glacier atop bedrock (Boulton, 1978; Pelletier, 2008; Koppes and Montgomery, 2009; Thomson et al., 2010); former basal sediment bodies located around the present-day Lake Pukaki seem to indicate that Pukaki glacier was instead underlain by thick glacial till (Hart, 1996). Field data illustrate that fast-flowing glaciers atop sediment bodies can erode 10–100 mm yr^{-1} (Björnsson, 1996; Hallet et al., 1996), making erosional processes significant on timescales as short as a thousand years.

Previous work has suggested that glacial erosion can lead to a progressive decrease in glacier extent over time (Kaplan et al., 2009). A primary goal of this study is to investigate whether this process might help explain the retreat of Pukaki glacier between the early and late LGM, a ~10,000 year interval. Although models are available which specifically couple glacier flow and bed erosion (Oerlemans, 1984; MacGregor et al., 2000; Egholm et al., 2011), we use a simpler static model, which is commensurate with the data limitations. This enables a more controlled calculation of glacier response to bed profile changes, and inquiry into the relative importance of climate and changing bed profiles in having reduced the extent of the Pukaki glacier from early to late LGM.

2. Regional setting

The Southern Alps are aligned northeast to southwest along the western boundary of the South Island, New Zealand, with a well-defined divide between westward and eastward drainage, known as the Main Divide. Located in the central part of the Southern Alps and southeast of the Main Divide, the Pukaki catchment includes many of the highest peaks of the Southern Alps. Lake Pukaki occupies the partly infilled trough of a large LGM glacier, which is commonly referred to as the Pukaki glacier (Schaefer et al., 2006; Putnam et al., 2010a; Barrell et al., 2011). Four large valley glaciers exist in the present climate in the Pukaki headwaters; from longest to shortest, they are the Tasman, Murchison, Mueller and Hooker glaciers (Fig. 1). During the LGM, they coalesced with ice from much of the Ben Ohau Range as well as the Jollie valley to form the Pukaki glacier (Porter, 1975). After the termination of the LGM, progressively fewer tributaries provided ice flux to the main valley glacier. By 13 ka, when the Pukaki glacier produced the Lateglacial Birch Hill moraines (Putnam et al., 2010a), the glacier was fed primarily by coalesced ice from the Tasman, Murchison, Hooker and Muller catchments, with some ice input from the northern end of the Ben Ohau Range (Fig. 1). Since at least the mid-Holocene until recent years, the extent of these glaciers has changed minimally, and each exists independently (e.g. Schaefer et al., 2009). The modeling presented here focuses on the Pukaki glacier and its tributaries.

The modern mountain glaciers in the Pukaki catchment are wet-based, as illustrated by the extensive outwash plains extending down-valley from the terminal zones. They have equilibrium line altitudes (ELA, the elevation of the boundary between glacier accumulation and ablation areas) ranging from about 1800 m near the Main Divide to about 2200 m on the easternmost glaciers (Porter, 1975; Lamont et al., 1999).

2.1. Present-day climate

The only long-term climate record for the Pukaki catchment headwaters is the NIWA Mt. Cook Hermitage station[1] located at 43.7°S, 170.1°E, elev. 765 m a.s.l. A 1903–1999 climatology at this site has mean annual temperature of 8.5 °C, with the coldest temperatures occurring in July and the warmest in February. The annual range in monthly mean temperatures is 12.2 °C. The instrumental record at the station indicates an upward trend of 0.67 °C per 100 years (85% significance level).

The lapse rate in the Pukaki catchment has been estimated to be 7.2 °C km^{-1} by comparing temperatures between Mt. Cook Hermitage climate station and a temporary climate station located at Tasman Saddle (2340 m a.s.l.). The lapse rate ranged between 8.0 °C km^{-1} in October and 6.4 °C km^{-1} in February, but did not exhibit a clear seasonal cycle (Ruddell, 1995). A lapse rate of 7.2 °C km^{-1} is higher than those typically assumed for New Zealand (5–6.5 °C km^{-1} Oerlemans, 1997; Anderson et al., 2010; Golledge et al., 2012), and may be due to the lower relative humidity on the east side of the Southern Alps (Ruddell, 1995).

Precipitation patterns on the South Island are strongly affected by the Southern Alps (Henderson and Thompson, 1999). A dominant westerly circulation brings moist air masses onto land, leading to heavy orographic precipitation along the northwestern slopes of the Southern Alps and a steep precipitation gradient southeast down the Pukaki catchment (New Zealand Meteorological Service, 1985; Tait et al., 2006; Stuart, 2011, Fig. 2). In line with previous modeling studies (e.g. Golledge et al., 2012), we scale but do not

[1] Data available at http://cliflo.niwa.co.nz/.

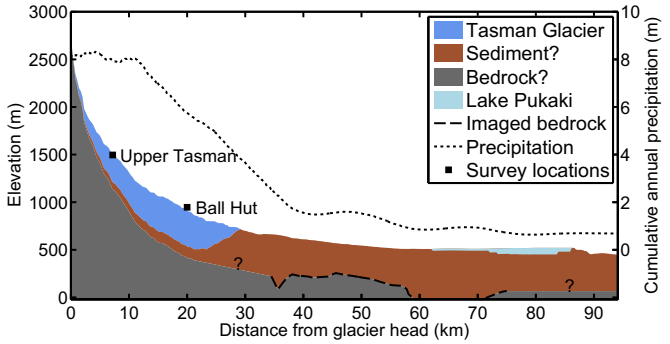

Fig. 2. The present-day setting of Tasman and Pukaki valley along the primary flowline. The ice/sediment and sediment/bedrock contacts are interpolated from surveys at Upper Pukaki and Ball Hut (Watson, 1995), and show a prominent terminal overdeepening. Lake Pukaki is enclosed by LGM moraines; lake bathymetry is from an echo sounding survey performed by Irwin (1972). Two seismic surveys (Kleffmann et al., 1998; Long et al., 2003) performed subparallel to the flowline show the elevation of the bedrock contact in the valley, which is hundreds of meters below the current surface in some places. Also shown is precipitation, which decreases rapidly with distance from the glacier head (New Zealand Meteorological Service, 1985; Tait et al., 2006; Stuart, 2011).

modify the pattern of precipitation, from Stuart (2011), when calculating LGM mass balance.

2.2. Geology and glacier landforms

The Southern Alps are being actively uplifted as a result of the oblique collision of the Australian and Pacific plates (Cox and Barrell, 2007). The basement rock of the Pukaki catchment consists of Mesozoic greywacke and argillite, metamorphosed to semischist close to the Main Divide of the Southern Alps. The rocks are deformed and fractured (Cox and Findlay, 1995), which has the effect of reducing rock strength and allowing for greater penetration of water into the rock, promoting mechanical and chemical weathering. Thus, the rock mass shatters and disintegrates relatively easily, shedding talus from the steep valley sides to the glacier ice or outlet stream transport systems. Overall erosion rates are suggested to be in a steady state with rock uplift, on the order of about 10 mm yr^{-1} (Adams, 1980). A similar value is estimated for sub-glacial erosion beneath modern Tasman Glacier (Kirkbride, 1989). There are extensive ice-marginal and down-valley outwash plains associated with the LGM glacier trough (Barrell et al., 2011), which suggest that the ice-age Pukaki glacier was, like the present-day glaciers in the Pukaki trough, wet-based (Golledge et al., 2012).

The bed of Tasman Glacier has been partially imaged via cross sections from seismic (Anderton, 1975) and gravity (Watson, 1995) surveys. Due to recent downwasting (Hochstein et al., 1995; Dykes et al., 2011) that has altered the surface elevation since the Anderton (1975) study, the elevation of the ice/sediment and sediment/bedrock interfaces is estimated based on the work of Watson (1995), and is shown in Fig. 2. The data indicate the existence of a terminal overdeepening, a feature proposed by Alley et al. (2003) to be the result of the stabilizing glacier erosion process of glaciohydraulic supercooling.

Seismic studies subparallel to the Pukaki basin provide estimates of the subsurface location of bedrock, which is presently covered by thick layers of sediment (Kleffmann et al., 1998; Long et al., 2003, Fig. 2). We use these estimates of bedrock elevation as a constraint on modeled bed profiles for the LGM (see Section 3.3).

Present-day glacier and surface elevation data are based on a 100-m resolution digital elevation model derived from 1986 photogrammetric contour and spot height data produced by Land Information New Zealand.

3. Model design

Pukaki glacier is simulated using a one-dimensional coupled mass balance–flowline model based on the SIA (Oerlemans, 1997). The bed profile boundary condition for the model is calculated using a modification of the coupled flow model (Anderson et al., 2004). Models are intentionally kept at low to intermediate complexity, due to limited data for model validation.

3.1. Flowline model

Pukaki glacier is modeled as a primary flowline with three incoming tributaries, as can be seen in Fig. 1. The flowline model is based on that used in Oerlemans (1997), with small modifications. The equation governing ice thickness, H, at each point on the flowline and on the tributaries is,

$$\frac{dH}{dt} = \frac{-1}{w_s \pm 2H\tan\theta}\frac{\partial}{\partial x}\left(D\frac{\partial h}{\partial x}\right) + M \tag{1}$$

where H is the ice thickness and h is the elevation of the ice surface. The glacier cross-section is approximated as a trapezoid, parameterized by the angle between the base and legs, θ, and the reference width, w_s, both of which are taken from the moraine record. The parameters θ and w_s can change along the flowline and tributaries. M is the mass balance, calculated via the Positive Degree Day (PDD) model in Section 3.2. D is the diffusivity, defined as,

$$D = (w_s \pm H\tan\theta)\left(f_d\gamma H^{n+2}\left(\frac{\partial h}{\partial x}\right)^{n-1} + f_s\gamma H^n\left(\frac{\partial H}{\partial x}\right)^{n-1}\right),$$
$$\gamma = (\rho_i g)^n \tag{2}$$

where n is Glen's constant. The diffusivity depends on the parameters f_s and f_d, which control sliding velocity and deformation, respectively. The prescription of the flow parameters is discussed in Section 3.3; values of these and all other model parameters are in Table 1.

The boundary condition of each tributary is the surface elevation of the closest point on the main flowline. Mass can therefore be transported in either direction between tributaries and trunk, depending on the sign of the ice flux calculated at the last point in the tributary. In the LGM climates considered here, the tributaries add mass to the trunk.

The spatial resolution of the model, Δx, is 300 m. The timestep, Δt, is adaptive to allow for both computational efficiency and numerical stability, and is calculated as (Hindmarsh, 2001),

Table 1
Values for the constants used in the mass balance and flowline models. L_f, ρ_w and ρ_i are physical constants; all others are calculated or taken from measurements.

Name	Var. name	Value	Units
Degree day factor (snow)	DDF_{snow}	3.4×10^{-3}	m.w.e. PDD^{-1}
Degree day factor (ice)	DDF_{ice}	7.4×10^{-3}	m.w.e. PDD^{-1}
Insolation factor	J	10^{-4}	m.w.e. J^{-1}
Snow/rain threshold	T_{snow}	2	°C
Temperature variability	σ	4	°C
Insolation scaling factor	S	0.03	°C $(W\ m^{-2})^{-1}$
Lag	ϕ	26	days
Latent heat of melting of water	L_f	3.34×10^5	J kg^{-1}
Density of water	ρ_w	1×10^3	kg m^{-3}
Density of ice	ρ_i	921	kg m^{-3}
Deformation parameter	f_d	3.7×10^{-22}	$Pa^{-3}\ s^{-1}$
Sliding parameter	f_s	1.2×10^{-17}	$m^2\ Pa^{-3}\ s^{-1}$
Glen's flow constant	n	3	

$$\Delta t = \frac{\Delta x^2}{2n \ \max(\mathrm{abs}(-UH/(\mathrm{d}h/\mathrm{d}x)))}, \quad \Delta t_{\max} = 20 \text{ days}, \tag{3}$$

where U is ice velocity, and all other variables are as above.

3.2. Mass balance

Surface mass balance is calculated using a PDD model, which relates melt to air temperature. Air temperature is a strong predictor of melt because incoming longwave radiation and turbulent heat exchange are important terms in the melt energy budget, and are closely related to 2-m air temperature (Ohmura, 2001). While PDDs are traditionally defined as the sum over time of the number of degrees above 0 °C for each day (e.g. Braithwaite, 1995; Hock, 2003), improved methods have been developed for calculating the number of PDDs from the climatological annual temperature cycle, $T(t)$. The seasonal cycle in temperature in the model is determined by insolation and the atmosphere lapse rate:

$$T(x,t) = SI(t-\phi)' + T(x)_{\mathrm{mean}}. \tag{4}$$

$I(t-\phi)'$ is the insolation anomaly from the annual mean, with a 26-day lag, ϕ, consistent with the present-day lag between insolation and temperature in and around the Pukaki catchment. S is the scaling factor controlling the annual temperature range, and $T(x)_{\mathrm{mean}}$ is the annual mean temperature at each point along the flowline and tributaries. Modeling temperature via a scaling and shifting of insolation captures 97% of the variance of the present-day climatological seasonal cycle at the Mt. Cook Hermitage climate station. Insolation is calculated as a function of latitude, day, and years before present according to astronomical geometry (Berger and Loutre, 1991).[2] The profile of temperature along the flowline and tributaries is determined by the lapse rate and the surface elevation at each point x, extrapolated from the temperature at the Mt. Cook Hermitage climate station (elev. 765 m a.s.l.).

We calculate PDDs as (Calov and Greve, 2005),

$$\mathrm{PDD}(x) = \int_{t1}^{t2} \mathrm{d}t \left[\frac{\sigma}{\sqrt{2\pi}} \exp\left(-\frac{T(x,t)^2}{2\sigma^2} \right) + \frac{T(x,t)}{2} \left(-\frac{T(x,t)}{\sqrt{2}\sigma} \right) \right] \tag{5}$$

where $[t1, t2]$ is the time period over which the PDDs are calculated, σ is the standard deviation of the temperature from that cycle, taking into account the diurnal cycle and stochastic temperature variations, and $T(x,t)$ is the annual cycle in temperature from Equation (4). While the number of PDDs can, in theory, be calculated over any time period, accuracy decreases with increasing temporal resolution (Hock, 2003).

The scaling factor between PDDs and melt is defined as the Degree Day Factor (DDF). In this work, two different DDFs are used, $\mathrm{DDF_{snow}}$ and $\mathrm{DDF_{ice}}$, reflecting the different melt rates for snow and ice due to their differing material properties, including albedo and the role of re-freezing. This requires calculating PDD values on shorter than annual timescales in order to take into account the seasonal cycle in snow accumulation; here, the calculation is done by calendar month. We also introduce a term directly relating melt to incoming solar radiation, which allows for a more accurate representation of the climate sensitivity of a glacier (Oerlemans, 2001). The model for annual melt can be written as,

$$\mathrm{melt}(x) = J \sum_{\mathrm{day}=1}^{365} \frac{I^+_{\mathrm{day}} \mathrm{d}t}{L_f \rho_w} + \sum_{\mathrm{month}=1}^{12} \mathrm{PDD}(x)_{\mathrm{month}} \mathrm{DDF}(x)_{\mathrm{month}}, \tag{6}$$

where $\mathrm{DDF}(x)_{\mathrm{month}} \in \{\mathrm{DDF_{snow}}, \mathrm{DDF_{ice}}\}$ is a function of space as well as month, so Equation (6) is applied at each point along the flowline and tributaries. Points are considered to be snow-covered if there has been snow accumulation for at least half of the month, and they are considered to be ice-covered otherwise. Following Huybers (2006), insolation contributes to melt only on days during which the daily mean is greater than 225 W $\mathrm{m^{-2}}$, and I^+_{day} is set to zero otherwise; for the latitude of Pukaki glacier, this correlates with days above freezing. L_f is the latent heat of melting for water, ρ_w is the density of water, $\mathrm{d}t$ is the number of seconds in a day, and J is the sensitivity of melt to solar insolation.

Accumulation is calculated using a snow/rain threshold, T_{snow}, below which precipitation is assumed to fall as snow. The spatial pattern of annual cumulative precipitation over both the main flowline (Fig. 2) and the tributaries (not shown) is set to the present-day based on Stuart (2011), but can be scaled uniformly. We do not include a seasonal cycle in precipitation itself; however, only snow, occurring when $T(x,t) \leq T_{\mathrm{snow}}$, contributes mass to the glacier. Snow that falls either on the glacier or in the catchment areas adds to glacier mass. Mass balance, M, is the difference between accumulation and melt.

The mass balance model is tuned to match available mass balance measurements on present-day Tasman Glacier (Chinn, 1994; Kirkbride, 1995; Purdie et al., 2011), which span the time period 1966 to 2009. The mass balance measurements are generally sparse for a given year (with the exception of 2008), and in order to utilize them, we assume that collectively they characterize the local climatology. This assumption is reinforced by the observation that the measurements present a consistent picture of mass balance that can be modeled using a single set of model parameters (see Fig. 3).

Based on previous work in New Zealand or in similar environments, the lapse rate in the mass balance model is set to 7.2 °C $\mathrm{km^{-1}}$ (Ruddell, 1995), $\mathrm{DDF_{snow}}$ is set to 3.4 mm $\mathrm{day^{-1}}$ $\mathrm{^\circ C^{-1}}$ (Hock, 2003; Cutler and Fitzharris, 2005), and the snow/rain threshold, T_{snow}, is set to 2 °C (Barringer, 1989; Kerr, 2005). We tune the model to best match the measurements using the scaling factor for insolation, J, and $\mathrm{DDF_{ice}}$. These two parameters are adjusted independently to reduce the root mean square error ($\mathrm{RMSE} = (E[(M_{\mathrm{modeled}} - M_{\mathrm{measured}})^2])^{1/2}$) between the modeled and measured mass balance. Names and values of all model parameters are shown in Table 1.

We also calculate a range of reasonable values for the five model parameters in the PDD, first bracketed by values found in the literature (Barringer, 1989; Ruddell, 1995; Oerlemans, 2001; Hock, 2003; Kerr, 2005), and further refined by excluding values that lead to a RMSE larger the one e-folding length on either side of the minimum RMSE (Fig. 3). The range of reasonable mass balance curves for each parameter is shown in Fig. 3. The mass balance model is most sensitive to $\mathrm{DDF_{ice}}$, because most ablation occurs in regions not dominated by accumulation, but is also sensitive to lapse rate, because of the large elevation range spanned by Tasman Glacier.

Model parameters are assumed to be constant across time. This assumption is reasonable for $\mathrm{DDF_{snow}}$, $\mathrm{DDF_{ice}}$ and the insolation factor, J; it is unlikely that the relationship between heat and melt has changed over time. We note that lapse rate, however, is

[2] Code available at http://www.ncdc.noaa.gov/paleo/pubs/huybers2006b/huybers2006b.html.

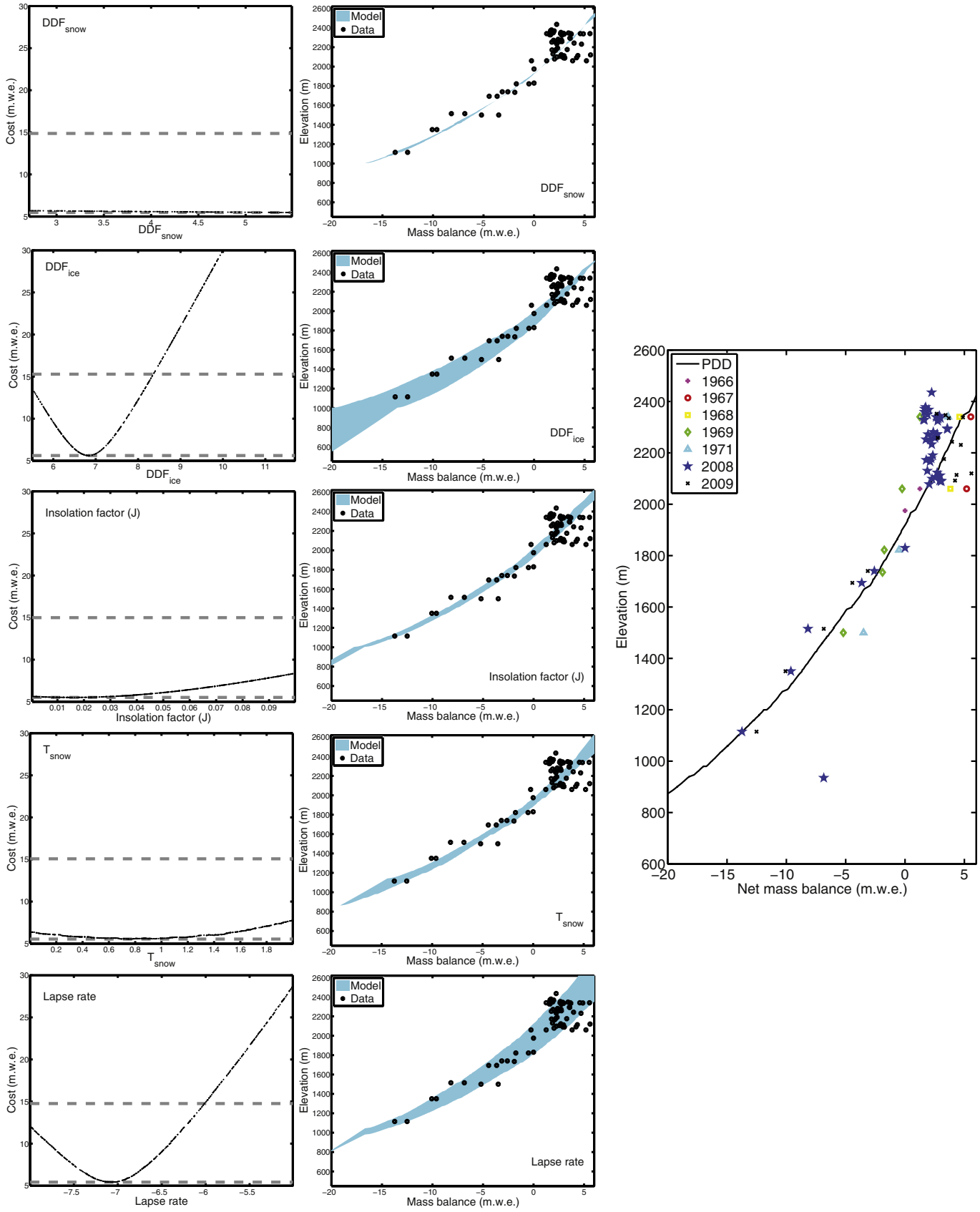

Fig. 3. *Left*: the RMSE for each of the five mass balance parameters. The cut-off for one e-folding length is shown in the gray dashed line. *Center*: the spread of mass balance profiles calculated by varying each of the five parameters within its reasonable range from the cost function. For each sensitivity test, one variable is changed and the other four are kept at the values in Table 1. *Right*: the modeled present-day mass balance profile using the PDD model, and available mass balance data. The mass balance curve is calculated statically, i.e. without being coupled to the flowline model. The PDD model does not include the effects of debris cover, which reduces ablation, accounting for the lowest-elevation data point.

dependent on relative humidity, which has likely changed between the LGM and today (e.g. Rojas et al., 2009), and the snow/rain threshold may also be sensitive to humidity (Kienzle, 2008) and temperature (Yang et al., 1997).

3.3. Bed profile model

Three models were considered for the purposes of calculating bed profiles: perfect plasticity, theoretical erosion, and mass flux balance. We use the third model in all future analysis, but briefly present the first two for comparison. Each model has at least one tuning parameter, the value of which must be determined by a constraint, for which we use available seismic data. The seismically-inferred bedrock surface (Section 2.2) is interpolated to the flowline using a 'nearest neighbor' approach, taking into account the difference in elevation between the flowline and the seismic line, and the calculated bed profiles are restricted to be above the inferred bedrock surface. This constraint assumes that the bedrock surface has not been substantially uplifted since the LGM.

3.3.1. Model 1

The perfect plasticity model, previously used by Oerlemans and Van der Veen (1984), can be used to calculate the bed profile, b, from surface height, h, and the yield stress, τ_y, as

$$b = h - \frac{\tau_y}{\rho_i g \dfrac{\mathrm{d}h}{\mathrm{d}x}}, \tag{7}$$

where ρ_i is ice density and g is the acceleration due to gravity. The assumption of perfect plasticity is known to be incorrect – it is the extreme case when Glen's flow constant goes to infinity (Oerlemans, 2001) – but offers a first approximation. The value of τ_y is the tuning parameter in this simple model that controls ice thickness, since surface height and slope can be measured. The model has an inverse dependence on the surface slope, so amplifies any surface roughness in the estimated profile, leading to the most unrealistic bed profile. For this reason, we do not strictly constrain the modeled bed profile to be above the bedrock surface, and instead take the value of τ_y as 10^5 Pa, consistent with that used by Oerlemans (1997).

3.3.2. Model 2

A second model for placing constraints on glacier beds was proposed by Anderson et al. (2006), and depends on the hypothesized proportionality of mass flux and erosion. For a one-dimensional flowline in steady state, mass flux, Q, can be determined from mass balance, M, and width, w, as,

$$Q(x) = \int_0^x Mw \; \mathrm{d}x'. \tag{8}$$

The erosion rate is argued to vary more directly with ice discharge per unit width, Q/w, recognizing the additional forces exerted in a narrower valley over a broad one by a glacier with the same mass flux. The total magnitude of erosion is calculated as $\kappa Q/w$, where the tuning parameter, κ, is a function of the time available for erosive processes in the steady state and the structural integrity of the bed material. The profile of erosion is then removed from an idealized "initial" profile of a linear bed that connects the upper- and lower-most points along the current surface, following the approach of Anderson et al. (2006).

3.3.3. Model 3

The third model for the bed profile (Anderson et al., 2004) also depends on the idea that a glacier in steady-state must have a mass flux profile that peaks at its ELA and diminishes to zero at its terminus. Given a mass flux, the flowline model (Section 3.1) can be solved iteratively to find the corresponding equilibrium ice thickness. Mass flux is calculated from the PDD model (Section 3.2), and bed elevation is calculated as the difference between the Porter (1975) glacier surface reconstruction and the equilibrium ice thickness. The equilibrium ice thickness profile depends on the sliding and deformation parameters (f_d and f_s, see Section 3.1), and is more sensitive to these parameters than to the mass flux profile. Large flow parameters correspond to an easily flowing ice body with a smaller ice thickness (and higher elevation bed for a given surface profile), with the converse being true about small flow parameters.

The bed profiles calculated from the three models are shown in Fig. 4. Despite their differences, all modeled beds show either a prominent terminal overdeepening (Models 1 and 3) or an overdeepened trough (Model 2). The similarity between the models encourages confidence in the large-scale structure of the reconstructed bed. The bed produced from the mass flux model is used for the analyses reported here because it offers model consistency between the bed model and the coupled flowline model and it incorporates more information about the Pukaki glacier system than the other two models. The terminal overdeepening of the profile is consistent with field observations on other highly erosive glaciers (Alley et al., 2003). The same model and model parameters are used to estimate the bed profile of the three incoming tributaries, since the flowline and tributaries share a similar environment and we are not aware of any available seismic or gravity data to locate the bedrock–sediment transition elevation for the tributaries.

3.4. Model evaluation

The fit of the full model to the moraine data is evaluated in two ways. First, the location of the modeled glacier terminus ($x_{\text{model term.}}$) is compared to the location of the terminal moraine farthest downvalley ($x_{\text{term. moraine}}$). Second, the elevation of the terminal and lateral moraines, h_{data}, are compared to the modeled

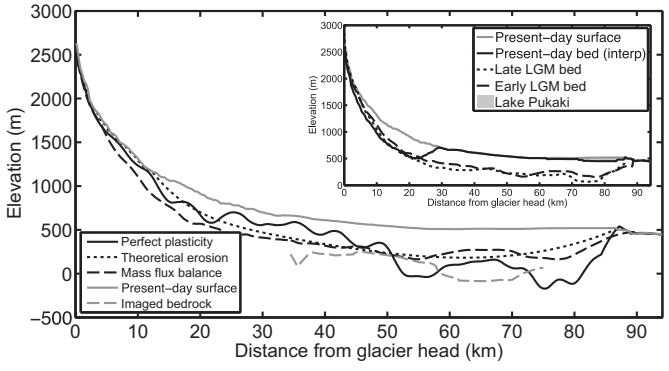

Fig. 4. Three models of the early LGM Pukaki glacier bed profile and the seismically-inferred buried bedrock surface (Kleffmann et al., 1998; Long et al., 2003), with the current surface for reference. All models exhibit a large-scale overdeepened trough. The mass flux balance profile is used in further analysis (see Section 3.3). *Inset*: a comparison between the early and late LGM, and present-day (interpolated, see Fig. 2) bed profiles. All exhibit terminal overdeepenings. The change between the LGM profiles and the present-day indicates that a large amount of sediment has been deposited in the glacial valley since the termination of the LGM.

glacier surface elevation, h_{model}. The latter criterion is quantified via a cost function,

$$C = \left[\sum_{x_{moraine}} (h_{data} - h_{model})^2 \right]^{1/2}. \quad (9)$$

The best-fit glacier profile is chosen as the one which minimizes C, with the requirement $x_{model\ term.} = x_{term.\ moraine}$.

4. Results: LGM climate reconstructions

4.1. Early LGM

A wide span of temperature and precipitation changes are considered for the early LGM, as shown in Fig. 5; three different climate states produce glacier profiles that align well with the moraine record. When precipitation is held to present-day levels, a temperature decrease of 7.0 °C from present reproduces early LGM Pukaki glacier length. For precipitation at levels that are 90% and 80% of present-day, decreases of 7.5 °C and 8.0 °C, respectively, are required. Simulations with smaller temperature decreases coupled with greater precipitation also reproduce the early LGM Pukaki glacier extent, but are biased toward slightly higher surface elevations. The profile from a 7.0 °C temperature decrease, holding precipitation at present-day levels, is shown in Fig. 6. Width and surface elevation are related in the model via the prescribed glacier cross-section, so the match to the moraine elevations also indicates a match to the glacier width indicated by the lateral moraines.

For temperature decreases ranging from 6.0 to 8.0 °C, a 20% increase (decrease) in precipitation can compensate for a 1 °C warmer (cooler) temperature. The magnitude of precipitation compensation seems to decrease to 15% for larger temperature changes (i.e. going from an 8.0–9.0 °C decrease). Conversely, a > 45% increase in precipitation from present levels is necessary to compensate for a temperature decrease of only 5.0 °C from present.

For all further analysis, we consider the perturbations from the 7 °C temperature decrease, present-day precipitation simulation, and will return to a discussion of precipitation changes in Section 5.

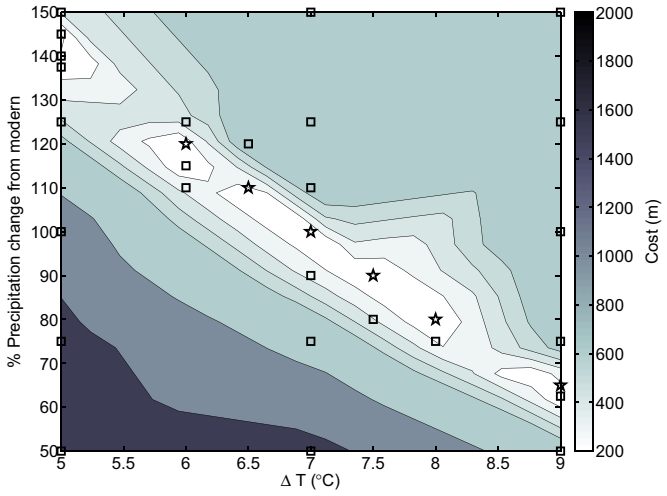

Fig. 5. Model fit to the moraine record, as measured by the cost function in Equation (9), for a range of temperature and precipitation values for the early LGM. Black squares and stars mark model simulations performed; stars indicate that the modeled glacier length matches the terminal moraine locations. Cost is linearly interpolated between model simulations.

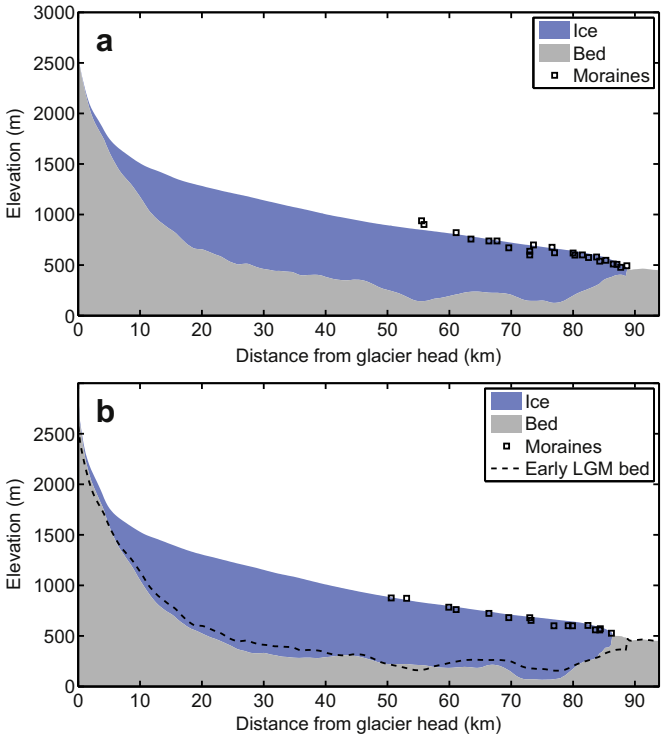

Fig. 6. The reconstructed profiles and moraine locations for the (a) early and (b) late LGM Pukaki glacier. Lateral and terminal moraines are indicated by black squares, and are taken from the geological map shown in Fig. 1 (Barrell et al., 2011). The early LGM bed is shown in a dotted line in the late LGM figure as a reference for the scale of bed profile change. A temperature decrease of 7.0 °C from present and present-day precipitation produce the early LGM profile; a mean warming of 0.1 °C from the early LGM with no change in precipitation produces the late LGM profile.

4.2. Sensitivity to mass balance parameters

The reasonable ranges of values for the five parameters in the PDD model, in Table 2, are used as a basis for determining the uncertainty in glacier length associated with the mass balance model.

Glacier length is most sensitive to the insolation melt factor, J, which scales melt directly with insolation, spans the largest range, and is the least constrained by earlier work. We thus exclude the larger temperature decrease required when $J \rightarrow 0.1$; the remaining temperature changes are 6.5–9.0 °C cooler than present. Interestingly, this range is skewed toward larger temperature decreases than the value of 7.0 °C cooler than present found using the set of parameters considered to be the most representative of the system with no changes in precipitation. Furthermore, the reconstructions from the two end member values of DDF_{snow} and T_{snow} bracket a range that does not overlap with the original 7.0 °C temperature decrease, indicating other non linearities in the model.

The effects of the annual range in temperature are briefly examined, which could result from changes in atmospheric

Table 2
The range of temperature decreases from present for the early LGM calculated from changing the five parameters in the model from their base values, shown in Table 1.

Constant name	Range (values)	Units	Range (ΔT, °C)
DDF_{snow}	$2.7–5.5 \times 10^{-3}$	m.w.e. PDD^{-1}	7.7–7.8
DDF_{ice}	$5.5–8.1 \times 10^{-3}$	m.w.e. PDD^{-1}	6.5–8.1
J	$10^{-4}–0.1$	m.w.e. J^{-1}	7.0–11.4
T_{snow}	0–2.5	°C	7.6–8.6
Lapse rate	6.2–8	°C km^{-1}	6.9–9.0

Table 3
Temperature changes from present for the LGM in New Zealand found in this and other studies.

Δ Temperature from present ° C	Location	Method and notes	Study
+0.5 to −1.9	Canterbury, South Island	Beetles (summer, LGM interstadial)	Marra et al. (2006)
+1.0 to −2.2	Canterbury, South Island	Beetles (winter, LGM interstadial)	Marra et al. (2006)
−0.9	Bay of Plenty, North Island	Foram-based winter SST	Samson et al. (2005)
−1.5	Bay of Plenty, North Island	Foram-based summer SST	Samson et al. (2005)
−1 to −3	Bay of Plenty, North Island	Foram-based SST	Barrows and Juggins (2005)
−1 to −4	Generalized central perhumid alpine region	Snow mass balance model	Rother and Shulmeister (2006)
−3 to −5	Central and northern NZ, east and west coasts	Foram-based SST	Barrows and Juggins (2005)
−4	North of Chatham Rise	Foram- and alkenone-based SST	Sikes et al. (2002)
−4	South of Chatham Rise	Alkenone-based SST	Sikes et al. (2002)
<−4	Auckland, North Island	Pollen assemblages	Sandiford et al. (2003)
−4.6	NZ average	Regional climate model	Drost et al. (2007)
−4 to −6	North of Chatham Rise	Foram-based SST	Weaver et al. (1998)
−5.3	Maratoto, North Island	Pollen assemblages	Wilmshurst et al. (2007)
−6.3 to −7.8	Lake Poukawa, North Island	Pollen assemblages	Shulmeister et al. (2001)
−6 to −6.5	Southern Alps ice field	Glacier modeling	Golledge et al. (2012)
−7 to −9	Southern NZ, east coast	Foram-based SST	Barrows and Juggins (2005)
−7 to −8 (−6.5 to −9)	Pukaki glacier system	Glacier modeling	This study
−6.5 to −9	Southern Alps, South Island	Regional climate modeling	Drost et al. (2007)
−8	South of Chatham Rise	Foram-based SST	Weaver et al. (1998)
−8	South of Chatham Rise	Foram-based SST	Sikes et al. (2002)

circulation patterns. An increased range in temperature, i.e. both warmer summers and cooler winters, leads to decreased glacier length. Increasing the range of monthly mean annual temperature by 2 °C during the LGM requires a compensating additional cooling of 0.5 °C in order to maintain the same length.

4.3. Sensitivity to bed profile

The bed profile is constrained by the inferred bedrock surface, which is used as a lower bound on the calculated bed, as discussed in Section 3.3. The elevation of this surface is, however, uncertain because (1) it is projected from the edge of Lake Pukaki to its center, and (2) its depth depends on correct seismic wave velocity modeling. In order to test the sensitivity of the model to bed elevation, we recalculate the bed profile twice, with the seismically-inferred bedrock surface shifted vertically by ±200 m. Because the bed profile model involves adjustment of the flow parameters, both f_d and f_s change with each calculated bed. Lowering the bedrock surface by 200 m also yields a temperature reconstruction of 7.0 °C colder than present. While this may seem surprising, the flow parameters provide a link between the bed profile and the flowline model, which apparently allows for different bed profiles to lead to the same temperature reconstruction. The effect is slightly asymmetric: increasing the elevation of the bedrock constraint leads to a temperature reconstruction of 6.7 °C colder than present.

The model is minimally sensitive to the elevation of the bedrock constraint by design, since the flow parameters are calculated in tandem with the bed profile, as discussed in Section 3.3.3. This model insensitivity does not imply that a similar behavior occurs in the real world, however. The values of the flow parameters reflect physical characteristics of the glacier and its environment, such as ice viscosity, which would not necessarily be expected to change in tandem with the bed profile. Thus, the flow parameters are kept constant between the early and late LGM simulations to determine the influences of the bed geometry on glacier length.

4.4. Late LGM

The bed profile of the late LGM Pukaki glacier is calculated using the mass flux method described in Section 3.3. This method produces a late LGM glacier bed that is generally lower than the early LGM glacier bed, consistent with expectations that glacial erosion will be progressive over time. The early LGM equilibrium glacier thickness is applied as an initial condition for the late LGM glacier simulations. From this position, the glacier requires only a 0.1 °C warming from the early LGM climate in order to retreat 2700 m from the early LGM to the late LGM ice configuration. The resulting glacier profile is shown in Fig. 6. While we do not simulate the early to late LGM transition for all of the reconstructed early LGM Pukaki glacier profiles (using different parameter sets), it can be assumed that the result would be similar.

We note that this reduction in Pukaki glacier extent from early to late LGM occurs due to a combination of changing the bed profile and increasing the temperature. Modeling allows the two effects to be deconvolved; an increase in temperature of 0.1 °C with a fixed bed leads to a decrease in glacier length of 300 m, while changing the bed profile with constant temperature leads to a decrease of 1200 m. The two effects apparently combine nonlinearly, to produce the length change of 2700 m that is consistent with the moraine record.

5. Discussion and conclusions

Glacier extent is controlled by mass balance, glacier flow dynamics, and the characteristics and geometry of the glacier bed. We have used a simple coupled mass balance–flowline model, in conjunction with a static model for bed profiles, to gain a better understanding of New Zealand LGM climate and the influence of glacier erosion on glacier length. The use of any simple model introduces an inherent bias in the results, but allows for a greater examination of model sensitivity and helps to prevent model overfitting.

Throughout the work, two important assumptions were made regarding the environment of Pukaki glacier.

First, we assume that the present-day westerly-wind-driven rainshadow precipitation regime is also representative of the LGM. While there is some evidence of greater southerly flow during the LGM (Drost et al., 2007), the precipitation pattern in the Pukaki catchment is influenced primarily by the combination of a westerly circulation and orographic effects, both of which would have remained important at the LGM. Additionally, we do not perform all model sensitivity tests with precipitation changes, largely because previous studies disagree about LGM precipitation in New Zealand (e.g. Hellstrom et al., 1998; Williams et al., 2005) and the one-dimensional model does not distinguish sufficiently between temperature and precipitation effects to provide additional insight.

Second, although the mass balance of present-day Tasman Glacier is heavily influenced by debris cover, which insulates against melt unless the cover is very thin (e.g. Nakawo and Young, 1981), we do not consider debris-cover effects in this study. Surface debris cover was likely to have been minimal on the Pukaki glacier during the LGM because Pukaki glacier extended out from the Main Divide into a region where rates of uplift and erosion are lower than those on slopes immediately surrounding present-day Tasman Glacier (Kirkbride and Matthews, 1997; Little et al., 2005), and snow or ice covered a greater proportion of the catchment area, reducing the source area for sub-aerial debris. These two factors, combined with the greater ice flux inherent for a larger glacier, suggest that the ratio of debris to ice flux was much smaller than present during the LGM, which typically corresponds to less surface debris cover (Brazier et al., 1998). Minimal surface debris cover is consistent with the existence of linear lateral moraines, which extend over tens of kilometers and are geographically separated from the glacial outwash plain and Lake Pukaki, as opposed to the hummocky moraines that would be expected from a debris covered glacier (Hambrey, 1994).

The LGM climate state found to be consistent with the Pukaki moraine record is within the range found in previous studies using various proxies, although our LGM temperature estimate is notably cooler, relative to modern conditions, than the majority of temperature estimates from previous studies (Table 3). One reason for this may be a latitudinal gradient in temperature change, since New Zealand spans almost 13 degrees of latitude. Sea surface temperature (SST) reconstructions indicate larger temperature decreases, relative to modern, in the southernmost parts of New Zealand than the northernmost. Paleoecological and modeling studies also indicate that the north–south temperature gradient may hold on land, with the exception of Shulmeister et al. (2001) and Rother and Shulmeister (2006). The reconstruction from the former has been questioned (Lorrey et al., 2012) and the latter focuses on a generalized rather than specific region. If these two studies are excluded, temperature decreases in the range of 4–5 °C have been found on the North Island, while temperature decreases of 5–9 °C have been found on the South Island.

In addition to exploring LGM climate states consistent with the Pukaki moraine record, we focus on the importance of evolving bed profiles in a temperate glacial environment. Three models produce LGM bed profiles with terminal overdeepenings, a feature lacking in many theoretical models for bed evolution (Hooke, 1991; MacGregor et al., 2000; Anderson et al., 2006) but observed in the field by Alley et al. (2003) and proposed as a stabilizing mechanism for glacier bed evolution. Alley et al. (2003) also suggested that the overdeepened bed should be 20–70% steeper than (and sloping in the opposite direction from) the overlying ice–air interface, which is broadly consistent with the LGM equilibrium surface and bed profiles. The presence of a terminal overdeepening in the present bed as well as those modeled for the LGM further indicates that it may be a persistent feature.

Bed topography is important to consider because erosion of the glacier bed can lead to glacier retreat without a change in climate, as shown here and previously suggested by Kaplan et al. (2009). Changing only the bed profile between the early and late LGM leads to a decrease in glacier extent of over 1 km; an additional, small warming is required for continued retreat to the late LGM moraine locations. Notably, when the bed profile and temperature changes are considered independently, the glacier length change due to erosion of the bed (1200 m) is four times larger than the length change due to warming (300 m). The two effects combine non-linearly for a total retreat of 2700 m. It is thus important to consider both processes when estimating climate changes through the moraine record in order to avoid an overestimation of the climate change required between different ice limits.

This study has illustrated the value of undertaking glacier modeling with an equal eye toward climatic forcing and glacier bed profile evolution. This is particularly important in environments, such as the Southern Alps, subject to active erosion and the rapid transport and deposition of sediment. We acknowledge the various uncertainties surrounding these environmental factors by employing a simple static model of bed topography, although the future development of more complex models would doubtless lead to an improved understanding of glacier bed evolution. In conclusion, the prevalence of moraines at many locations globally, coupled with advances in dating technologies, encourages the use of glacier modeling to obtain glaciological paleoclimate reconstructions. Geomorphologically-based glacier reconstructions provide an important complement to marine SST and polar ice core records in the quest to understand the spatial as well as temporal patterns of past climate changes.

Acknowledgments

Funding for KAM was provided through the Packard Foundation and the NSF GRFP. ANM and BMA were supported by NZ MSI Program “ANZICE”. DJAB was supported by the NZ MSI Program “Margins – Source to sink”. KAM thanks Alice Doughty, Mike Kaplan, George Denton and Aaron Putnam for their insight into the Pukaki catchment, Nicholas Golledge for discussions regarding glacier modeling, Euan Smith and Richard Alley for comments on a previous version of this work, Peter Huybers for manuscript comments and revisions, and Andreas Vieli and Ann Rowan for their constructive reviews.

References

Adams, J., 1980. Contemporary uplift and erosion of the Southern Alps, New Zealand: summary. Bulletin of the Geological Society of America 91, 2–4.
Alley, R.B., Lawson, D.E., Larson, G.J., Evenson, E.B., Baker, G.S., 2003. Stabilizing feedbacks in glacier-bed erosion. Nature 424, 758–760.
Alloway, B.V., Lowe, D.J., Barrell, D.J.A., Newnham, R.M., Almond, P.C., Augustinus, P.C., Bertler, N.A.N., Carter, L., Litchfield, N.J., McGlone, M.S., Shulmeister, J., Vandergoes, M.J., Williams, P.W., 2007. Towards a climate event stratigraphy for New Zealand over the past 30 000 years (NZ-INTIMATE project). Journal of Quaternary Science 22, 9–35.
Anderson, B.M., Hindmarsh, R.C.A., Lawson, W.J., 2004. A modelling study of the response of Hatherton Glacier to Ross Ice Sheet grounding line retreat. Global and Planetary Change 42, 143–153.
Anderson, B.M., Mackintosh, A.N., Stumm, D., George, L., Kerr, T., Winter-Billington, A., Fitzsimons, S., 2010. Climate sensitivity of a high-precipitation glacier in New Zealand. Journal of Glaciology 56, 114–128.
Anderson, R.S., Molnar, P., Kessler, M.A., 2006. Features of glacial valley profiles simply explained. Journal of Geophysical Research 111, F01004.
Anderton, P.W., 1975. Tasman Glacier 1971–73. In: Hydrological Research Annual Report 33. Ministry of Works and Development for the National Water and Soil Conservation Organisation, Wellington, pp. 28.
Baral, D.R., Hutter, K., Greve, R., 2001. Asymptotic theories of large-scale motion, temperature, and moisture distribution in land-based polythermal ice sheets: a critical review and new developments. Applied Mechanics Reviews 54, 215–256.
Barrell, D.J.A., 2011. Quaternary glaciers of New Zealand. In: Ehlers, J., Gibbard, P., Hughes, P. (Eds.), Quaternary Glaciations – Extent and Chronology, Part IV –

a Closer Look. Developments in Quaternary Science, vol. 15. Elsevier, Amsterdam, pp. 1047–1064.
Barrell, D.J.A., Andersen, B.G., Denton, G.H., 2011. Glacial Geomorphology of the Central South Island, New Zealand. In: GNS Science Monograph, vol. 27. GNS Science, Lower Hutt, New Zealand. 81 pp + map (5 sheets) + legend (1 sheet).
Barringer, J.R.F., 1989. A variable lapse rate snowline model for the remarkables, Central Otago, New Zealand. Journal of Hydrology (NZ) 28, 32–46.
Barrows, T.T., Juggins, S., 2005. Sea-surface temperatures around the Australian margin and Indian Ocean during the Last Glacial Maximum. Quaternary Science Reviews 24, 1017–1047.
Berger, A., Loutre, M.F., 1991. Insolation values for the climate of the last 10 million years. Quaternary Science Reviews 10, 297–317.
Björnsson, H., 1996. Scales and rates of glacial sediment removal: a 20 km long and 300 m deep trench created beneath Breiðamerkurjökull during the Little Ice Age. Annals of Glaciology 22, 141–146.
Boulton, G.S., 1978. Processes of glacier erosion on different substrata. In: Symposium on Glacier Beds: the Ice-rock Interface. Journal of Glaciology, Carleton University, Ottawa, Ontario, pp. 15–38.
Boulton, G.S., Jones, A.S., 1979. Stability of temperate ice caps and ice sheets resting on beds of deformable sediment. Journal of Glaciology 24, 29–43.
Braithwaite, R.J., 1995. Positive degree-day factors for ablation on the Greenland ice sheet studied by energy-balance modelling. Journal of Glaciology 41, 153–160.
Brazier, V., Kirkbride, M.P., Owens, I.F., 1998. The relationship between climate and rock glacier distribution in the Ben Ohau Range, New Zealand. Geografiska Annaler: Series A, Physical Geography 80, 193–207.
Calov, R., Greve, R., 2005. A semi-analytical solution for the positive degree-day model with stochastic temperature variations. Journal of Glaciology 51, 173–175.
Chinn, T.J.H., 1994. Snow and Ice Balance Measurements from the Tasman Glacier, Waitaki Catchment, New Zealand. Institute of Geological and Nuclear Sciences Client Report 413399.22, Prepared for the Electricity Corporation of New Zealand.
Cox, S., Barrell, D.J.A., 2007. Geology of the Aoraki Area, Institute of Geological and Nuclear Sciences 1:250,000 Geological Map 15. GNS Science, Lower Hutt, New Zealand, 1 Sheet, pp. 71.
Cox, S.C., Findlay, R.H., 1995. The main divide fault zone and its role in formation of the Southern Alps, New Zealand. New Zealand Journal of Geology and Geophysics 38, 489–499.
Cutler, E.S., Fitzharris, B., 2005. Observed surface snowmelt at high elevation in the Southern Alps of New Zealand. Annals of Glaciology 40, 163–168.
Drost, F., Renwick, J., Bhaskaran, B., Oliver, H., McGregor, J., 2007. A simulation of New Zealand's climate during the Last Glacial Maximum. Quaternary Science Reviews 26, 2505–2525.
Dykes, R.C., Brook, M.S., Robertson, C.M., Fuller, I.C., 2011. Twenty-first century calving retreat of Tasman Glacier, Southern Alps, New Zealand. Arctic, Antarctic, and Alpine Research 43, 1–10.
Egholm, D.L., Pedersen, V.K., Knudsen, M.F., Larsen, N.K., 2011. Coupling the flow of ice, water, and sediment in a glacial landscape evolution model. Geomorphology 141,142, 47–66.
Golledge, N.A., Mackintosh, A.N., Anderson, B.M., Buckley, K.M., Doughty, A.M., Barrell, D.J.A., Denton, G.H., Vandergoes, M.J., Andersen, B.G., Schaefer, J.M., 2012. Last Glacial Maximum climate in New Zealand inferred from a modelled Southern Alps icefield. Quaternary Science Reviews 46, 30–45.
Hallet, B., Hunter, L., Bogen, J., 1996. Rates of erosion and sediment evacuation by glaciers: a review of field data and their implications. Global and Planetary Change 12, 213–235.
Hambrey, M.J., 1994. Glacial Environments. University of British Columbia Press, Vancouver, British Columbia.
Hart, J.K., 1996. Proglacial glaciotectonic deformation associated with glaciolacustrine sedimentation, Lake Pukaki, New Zealand. Journal of Quaternary Science 11, 149–160.
Hellstrom, J., McCulloch, M., Stone, J., 1998. A detailed 31,000-year record of climate and vegetation change, from the isotope geochemistry of two New Zealand speleothems. Quaternary Research 50, 167–178.
Henderson, R.D., Thompson, S.M., 1999. Extreme rainfalls in the Southern Alps of New Zealand. New Zealand Journal of Hydrology 38, 309–330.
Hindmarsh, R.C.A., 2001. Notes on basic glaciological computational methods and algorithms. In: Straughan, B., Greve, R., Ehrentraut, H., Wang, Y. (Eds.), Continuum Mechanics and Applications in Geophysics and the Environment. Springer-Verlag, Berlin, pp. 222–249.
Hindmarsh, R.C.A., 2006. Stress gradient damping of thermoviscous ice flow instabilities. Journal of Geophysical Research 111, B12409.
Hochstein, M.P., Claridge, D., Henrys, S.A., Pyne, A., Nobes, D.C., Leary, S.F., 1995. Downwasting of the Tasman Glacier, South Island, New Zealand: changes in the terminus region between 1971 and 1993. New Zealand Journal of Geology and Geophysics 38, 1–16.
Hock, R., 2003. Temperature index melt modelling in mountain areas. Journal of Hydrology 282, 104–115.
Hooke, R.L.E.B., 1991. Positive feedbacks associated with erosion of glacial cirques and overdeepenings. Bulletin of the Geological Society of America 103, 1104–1108.
Huybers, P., 2006. Early Pleistocene glacial cycles and the integrated summer insolation forcing. Science 313, 508–511.
Irwin, J., 1972. Sediments of Lake Pukaki, South Island, New Zealand. New Zealand Journal of Marine and Freshwater Research 6, 482–491.
Kamb, B., Echelmeyer, K., 1986. Stress-gradient coupling in glacier flow. I: longitudinal averaging of the influence of ice thickness and surface slope. Journal of Glaciology 32, 267–284.
Kaplan, M.R., Hein, A.S., Hubbard, A., Lax, S.M., 2009. Can glacial erosion limit the extent of glaciation? Geomorphology 103, 172–179.
Kaplan, M.R., Schaefer, J.M., Denton, G.H., Barrell, D.J.A., Chinn, T.J.H., Putnam, A.E., Andersen, B.G., Finkel, R.C., Schwartz, R., Doughty, A.M., 2010. Glacier retreat in New Zealand during the Younger Dryas stadial. Nature 467, 194–197.
Kerr, T.R., 2005. Snow Storage Modelling in the Lake Pukaki Catchment, New Zealand: an Investigation of Enhancements to the Snowsim Model. Masters' thesis, University of Canterbury, Christchurch.
Kienzle, S.W., 2008. A new temperature based method to separate rain and snow. Hydrological Processes 22, 5067–5085.
Kirkbride, M., 1989. The Influence of Sediment Budget on Geomorphic Activity of the Tasman Glacier, Mount Cook National Park, New Zealand. Doctoral thesis, University of Canterbury, Christchurch.
Kirkbride, M., Matthews, D., 1997. The role of fluvial and glacial erosion in landscape evolution: the Ben Ohau Range, New Zealand. Earth Surface Processes and Landforms 22, 317–327.
Kirkbride, M.P., 1995. Relationships between temperature and ablation on the Tasman Glacier, Mount Cook National Park, New Zealand. New Zealand Journal of Geology and Geophysics 38, 17–27.
Kleffmann, S., Davey, F., Melhuish, A., Okaya, D., Stern, T., 1998. Crustal structure in the central South Island, New Zealand, from the Lake Pukaki seismic experiment. New Zealand Journal of Geology and Geophysics 41, 39–49.
Koppes, M.N., Montgomery, D.R., 2009. The relative efficacy of fluvial and glacial erosion over modern to orogenic timescales. Nature Geoscience 2, 644–647.
Lamont, G.N., Chinn, T.J., Fitzharris, B.B., 1999. Slopes of glacier ELAs in the Southern Alps of New Zealand in relation to atmospheric circulation patterns. Global and Planetary Change 22, 209–219.
Le Meur, E., Gagliardini, O., Zwinger, T., Ruokolainen, J., 2004. Glacier flow modelling: a comparison of the Shallow Ice approximation and the full-stokes solution. Comptes Rendus Physique 5, 709–722.
Leysinger Vieli, G.J., Gudmundsson, G.H., 2004. On estimating length fluctuations of glaciers caused by changes in climatic forcing. Journal of Geophysical Research: Earth Surface 109, F01007.
Little, T.A., Cox, S., Vry, J.K., Batt, G., 2005. Variations in exhumation level and uplift rate along the oblique-slip Alpine fault, central Southern Alps, New Zealand. Geological Society of America Bulletin 117, 707–723.
Long, D.T., Cox, S.C., Bannister, S., Gerstenberger, M.C., Okaya, D., 2003. Upper crustal structure beneath the eastern Southern Alps and the Mackenzie Basin, New Zealand, derived from seismic reflection data. New Zealand Journal of Geology and Geophysics 46, 21–40.
Lorrey, A.M., Vandergoes, M., Almond, P., Renwick, J., Stephens, T., Bostock, H., Mackintosh, A.N., Newnham, R., Williams, P.W., Ackerley, D., Neil, H., Fowler, A.M., 2012. Palaeocirculation across New Zealand during the Last Glacial Maximum at 21 ka. Quaternary Science Reviews 36, 189–213.
MacGregor, K.R., Anderson, R.S., Anderson, S.P., Waddington, E.D., 2000. Numerical simulations of glacial-valley longitudinal profile evolution. Geology 28, 1031–1034.
Marra, M.J., Shulmeister, J., Smith, E.G.C., 2006. Reconstructing temperature during the Last Glacial Maximum from Lyndon Stream, South Island, New Zealand using beetle fossils and maximum likelihood envelopes. Quaternary Science Reviews 25, 1841–1849.
Nakawo, M., Young, G.J., 1981. Field experiments to determine the effect of a debris layer on ablation of glacier ice. Annals of Glaciology 2, 85–91.
New Zealand Meteorological Service, 1985. Climatic Map Series. In: Part 6: Annual Rainfall, vol. 175. New Zealand Meteorological Service Miscellaneous Publication, Wellington, New Zealand.
Oerlemans, J., 1984. Numerical experiments on glacial erosion. Zeitschrift für Gletscherkunde und Glazialgeologie 20, 107–126.
Oerlemans, J., 1989. On the response of valley glaciers to climatic change. In: Glacier Fluctuations and Climatic Change: Proceedings of the Symposium on Glacier Fluctuations and Climatic Change, Held in Amsterdam, 1–5 June 1987. Kluwer, pp. 353–371.
Oerlemans, J., 1997. Climate sensitivity of Franz Josef Glacier, New Zealand, as revealed by numerical modeling. Arctic and Alpine Research 29, 233–239.
Oerlemans, J., 2001. Glaciers and Climate Change. A. A. Balkema Publishers, Rotterdam, Netherlands.
Oerlemans, J., Anderson, B.M., Hubbard, A., Huybrechts, P., Johannesson, T., Knap, W.H., Schmeits, M., Stroeven, A.P., Van de Wal, R.S.W., Wallinga, J., Zuo, Z., 1998. Modelling the response of glaciers to climate warming. Climate Dynamics 14, 267–274.
Oerlemans, J., Van der Veen, C.J., 1984. Ice Sheets and Climate. Reidel, Dordrecht.
Ohmura, A., 2001. Physical basis for the temperature-based melt-index method. Journal of Applied Meteorology 40, 753–761.
Pahnke, K., Zahn, R., Elderfield, H., Schulz, M., 2003. 340,000-year centennial-scale marine record of Southern Hemisphere climatic oscillation. Science 301, 948–952.
Pelletier, J.D., 2008. Glacial erosion and mountain building. Geology 36, 591–592.
Porter, S.C., 1975. Equilibrium-line altitudes of late Quaternary glaciers in the Southern Alps, New Zealand. Quaternary Research 5, 27–47.
Purdie, H., Anderson, B.M., Lawson, W., Mackintosh, A.N., 2011. Controls on spatial variability in snow accumulation on glaciers in the Southern Alps, New Zealand; as revealed by crevasse stratigraphy. Hydrological Processes 25, 54–63.

Putnam, A.E., Denton, G.H., Schaefer, J.M., Barrell, D.J.A., Andersen, B.G., Finkel, R.C., Schwartz, R., Doughty, A.M., Kaplan, M.R., Schlüchter, C., 2010a. Glacier advance in southern middle-latitudes during the Antarctic Cold Reversal. Nature Geoscience 3, 700–704.

Putnam, A.E., Schaefer, J.M., Barrell, D.J.A., Vandergoes, M., Denton, G.H., Kaplan, M.R., Finkel, R.C., Schwartz, R., Goehring, B.M., Kelley, S.E., 2010b. In situ cosmogenic 10Be production-rate calibration from the Southern Alps, New Zealand. Quaternary Geochronology 5, 392–409.

Rojas, M., Moreno, P., Kageyama, M., Crucifix, M., Hewitt, C., Abe-Ouchi, A., Ohgaito, R., Brady, E.C., Hope, P., 2009. The Southern Westerlies during the Last Glacial Maximum in PMIP2 simulations. Climate Dynamics 32, 525–548.

Rother, H., Shulmeister, J., 2006. Synoptic climate change as a driver of late Quaternary glaciations in the mid-latitudes of the Southern Hemisphere. Climate of the Past 2, 11–19.

Rowan, A.V., Plummer, M.A., Brocklehurst, S.H., Jones, M.A., Schultz, D.M. Drainage capture and discharge variations driven by glaciation in the Southern Alps, New Zealand. Geology, in press.

Ruddell, A.R., 1995. Recent Glacier and Climate Change in the New Zealand Alps. Doctoral thesis, School of Earth Sciences, University of Melbourne, Melbourne.

Samson, C.R., Sikes, E.L., Howard, W.R., 2005. Deglacial paleoceanographic history of the Bay of Plenty, New Zealand. Paleoceanography 20, 4017–4028.

Sandiford, A., Newnham, R., Alloway, B., Ogden, J., 2003. A 28 000–7600 cal yr BP pollen record of vegetation and climate change from Pukaki Crater, northern New Zealand. Palaeogeography, Palaeoclimatology, Palaeoecology 201, 235–247.

Schaefer, J.M., Denton, G.H., Barrell, D.J.A., Ivy-Ochs, S., Kubik, P.W., Andersen, B.G., Phillips, F.M., Lowell, T.V., Schlüchter, C., 2006. Near-synchronous interhemispheric termination of the Last Glacial Maximum in mid-latitudes. Science 312, 1510–1513.

Schaefer, J.M., Denton, G.H., Kaplan, M., Putnam, A., Finkel, R.C., Barrell, D.J.A., Andersen, B.G., Schwartz, R., Mackintosh, A.N., Chinn, T., Schlüchter, C., 2009. High-frequency Holocene glacier fluctuations in New Zealand differ from the northern signature. Science 324, 622–625.

Shulmeister, J., Shane, P., Lian, O.B., Okuda, M., Carter, J.A., Harper, M., Dickinson, W., Augustinus, P., Heijnis, H., 2001. A long late-Quaternary record from Lake Poukawa, Hawke's Bay, New Zealand. Palaeogeography, Palaeoclimatology, Palaeoecology 176, 81–107.

Sikes, E.L., Howard, W.R., Neil, H.L., Volkman, J.K., 2002. Glacial-interglacial sea surface temperature changes across the subtropical front east of New Zealand based on alkenone unsaturation ratios and foraminiferal assemblages. Paleoceanography 17, 1012–1024.

Solomon, S., Qin, D., Manning, M., Chen, Z., Marquis, M., Averyt, K.B., Tignor, M., Miller, H.L. (Eds.), 2007. Climate Change 2007: the Physical Science Basis. Contribution of Working Group I to the Fourth Assessment Report of the Intergovernmental Panel on Climate Change. Cambridge University Press, Cambridge.

Stuart, S.J., 2011. Observations and Modelling of Precipitation in the Southern Alps of New Zealand. Masters' thesis, Victoria University of Wellington, Wellington.

Tait, A., Henderson, R., Turner, R., Zheng, X., 2006. Thin plate smoothing spline interpolation of daily rainfall for New Zealand using a climatological rainfall surface. International Journal of Climatology 26, 2097–2115.

Thomson, S.N., Brandon, M.T., Tomkin, J.H., Reiners, P.W., Vásquez, C., Wilson, N.J., 2010. Glaciation as a destructive and constructive control on mountain building. Nature 467, 313–317.

Truffer, M., Echelmeyer, K.A., Harrison, W.D., 2001. Implications of till deformation on glacier dynamics. Journal of Glaciology 47, 123–134.

Watson, M.I., 1995. Geophysical and Glaciological Studies of the Tasman and Mueller Glaciers. Doctoral thesis, University of Auckland, Auckland.

Weaver, P.P.E., Carter, L., Neil, H.L., 1998. Response of surface water masses and circulation to late Quaternary climate change east of New Zealand. Paleoceanography 13, 70–83.

Williams, P.W., King, D.N.T., Zhao, J.X., Collerson, K.D., 2005. Late Pleistocene to Holocene composite speleothem ^{18}O and ^{13}C chronologies from South Island, New Zealand – did a global Younger Dryas really exist? Earth and Planetary Science Letters 230, 301–317.

Wilmshurst, J.M., McGlone, M.S., Leathwick, J.R., Newnham, R.M., 2007. A pre-deforestation pollen-climate calibration model for New Zealand and quantitative temperature reconstructions for the past 18 000 years BP. Journal of Quaternary Science 22, 535–547.

Yang, Z.L., Dickinson, R.E., Robock, A., Vinnikov, K.Y., 1997. Validation of the snow submodel of the biosphere-atmosphere transfer scheme with Russian snow cover and meteorological observational data. Journal of Climate 10, 353–373.